Geofísica Internacional (1997), Vol. 36, 3, pp. 139-159

The Victoria, Mexico, Earthquake of June 9, 1980

V.Wong, J. Frez and F. Suárez
Earth Sciences Division
CICESE, Ensenada, B.C., México.

Received: June 7, 1996; accepted: February 24, 1997

RESUMEN

El sismo de Victoria de junio 9 de 1980 ($M_L = 6.1$) ocurrió en el Valle de Mexicali cerca de la traza de la falla de Cerro Prieto con un mecanismo focal de fallamiento de rumbo con movimiento lateral derecho en un plano vertical. Se presentan los resultados obtenidos del análisis de datos locales concernientes a los efectos superficiales, localizaciones hipocentrales y mecanismos focales, tanto del evento principal como de la actividad de réplicas. No se observan en la superficie las evidencias de los desplazamientos ocasionados por la propagación de la fractura del evento principal. La actividad de réplicas se localizó al noroeste del epicentro del evento principal, concentrándose en pequeños grupos en o cerca del extremo noroeste de la falla Cerro Prieto. Algunas réplicas se localizaron al norte de donde termina la falla Cerro Prieto y hacia el extremo sureste de la falla Imperial. Sólo un pequeño número de réplicas fue localizado en los alrededores del evento principal y ocurrieron pocas horas despues de éste. La actividad de réplicas está localizada principalmente entre 3 y 8 km de profundidad, ubicándose la mayoría de ellas por debajo de la gruesa capa de sedimentos. La profundidad promedio de las réplicas generalmente decrece hacia el noroeste, alejándose del epicentro del evento principal, el cual se encuentra a 9 km de profundidad. Los mecanismos focales compuestos de las réplicas nos muestran un movimiento lateral derecho sobre un plano vertical con orientación N45°W para el grupo más cercano al evento principal, y fallamiento normal para el grupo en el extremo noroeste de la falla Cerro Prieto. Dos pequeños enjambres sísmicos ocurrieron pocas horas antes del evento principal.

PALABRAS CLAVE: Sismo de Victoria, actividad de réplicas, efectos por el sismo, Valle de Mexicali.

ABSTRACT

The Victoria earthquake of June 9, 1980 ($M_L = 6.1$), occurred in the Mexicali Valley near the trace of the Cerro Prieto fault with a focal mechanism consisting of a dextral strike-slip motion on a vertical fault. We present results from an analysis of local data concerning ground surface effects, epicenter locations, and focal mechanisms of the main shock and its aftershock activity. A field reconnaissance showed no clear ground surface displacement related to the main shock. The aftershocks occurred northwest of the main shock epicenter, in a few clusters at or near the northwest end of the Cerro Prieto fault. There was some aftershock activity north of the Cerro Prieto fault tip and towards the southeast end of the Imperial fault. Only a few aftershocks were located near the main shock; they occurred during the first few hours after the main event. The aftershock activity was mainly located between 3 and 8 km in depth, beneath the thick overlying sediments. The average depth of the aftershocks generally decreases to the northwest, away from the main epicenter which is at a depth of about 9 km. Composite focal mechanisms of the aftershocks show a right-lateral strike-slip motion on a vertical plane striking N45°W for the cluster near the main shock epicenter, and normal faulting for the cluster at the northwest end of the Cerro Prieto fault. Two small tightly clustered earthquake swarms occurred a few hours before the main shock.

KEY WORDS: Victoria Earthquake, aftershock activity, earthquake effects, Mexicali Valley.

1. INTRODUCTION

On June 9, 1980 an earthquake of magnitude (M_L) 6.1 occurred about 50 km southeast of the city of Mexicali, Baja California, Mexico. The preliminary location of this event was near the intersection of the Cerro Prieto fault with the Colorado river (Figure 1). The Victoria earthquake was part of a strong increase in seismicity that occurred in the Mexicali-Imperial Valley area from 1973 to 1981; this seismic activity included many swarms and another moderate magnitude event: the Imperial Valley earthquake of October 15, 1979 ($M_L = 6.4$). Aftershock locations of the Imperial Valley and Victoria earthquakes from the Southern California Catalog (SCC), are shown in Figure 2. Systematic errors of these locations are discussed in a later section.

Both aftershock sequences are mostly confined to a zone between the Imperial and Cerro Prieto faults, where several earthquake swarms occurred between 1973 and 1981; this is called the Mexicali Seismic Zone (Frez and González, 1987; see also Figures 1 and 2). This seismic zone is linked to the opening of the Gulf of California by the Cerro Prieto and the Imperial faults; it has been interpreted as a small spreading center (Lomnitz *et al.*, 1970; Elders *et al.*, 1972). The seismic activity between 1973 and 1983 associated with the Brawley (Johnson, 1979) and Mexicali seismic zones is shown as a time-distance plot in Figure 3; the data are from the SCC.

Thirteen hours after the Victoria earthquake, the first of ten seismological stations was installed to monitor the aftershock activity. The stations were operated by the University of California at San Diego (UCSD), Universidad Nacional Autónoma de México (UNAM), and Centro de Investigación Científica y de Educación Superior de Ensenada (CICESE). The temporary network consisted of

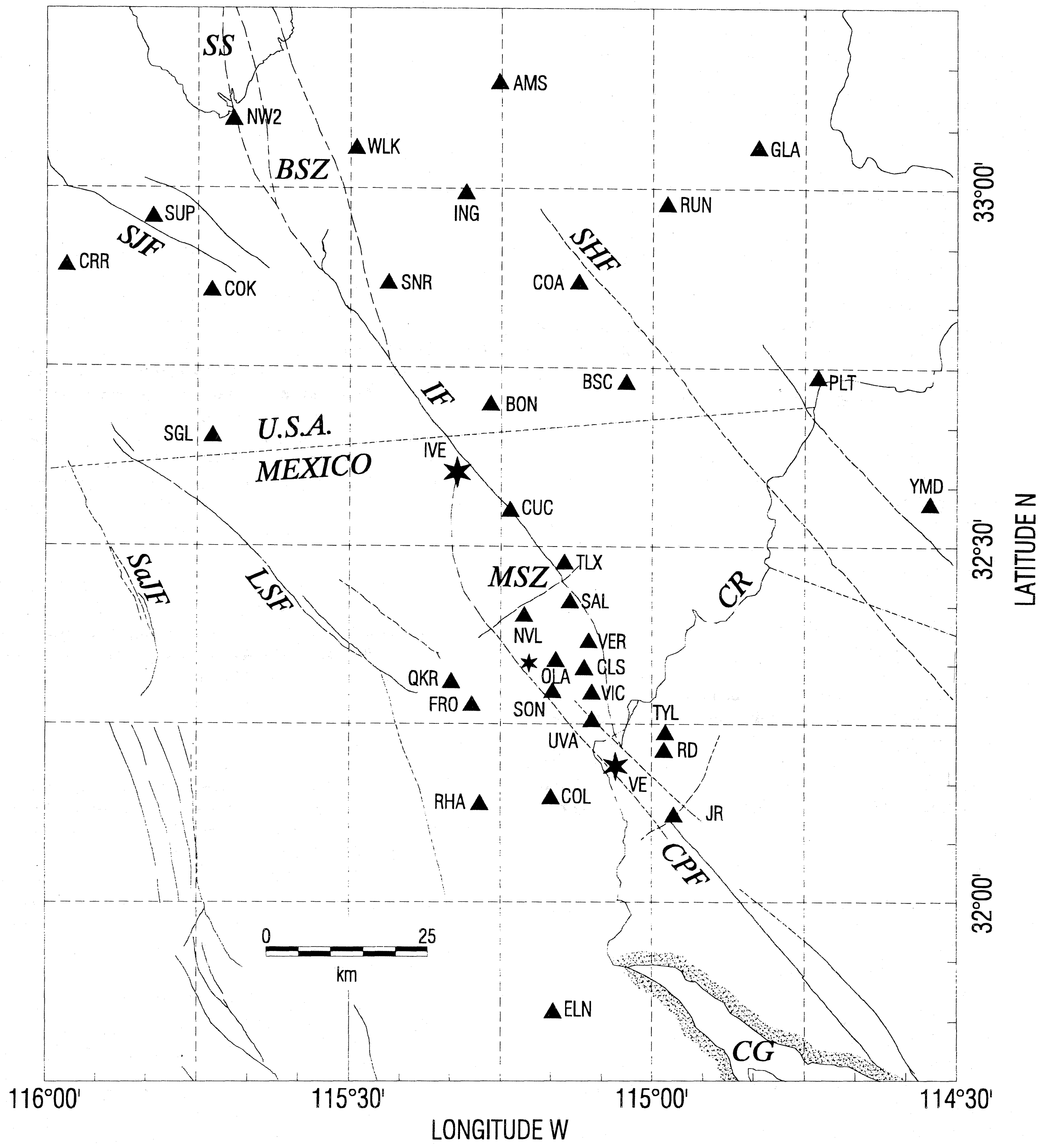

Fig. 1. Index map showing major faults, local and regional stations in the area of study. Solid stars, epicenters of the Imperial Valley earthquake (IVE) of October 15, 1979 (Chávez *et al.*, 1982) and the main shock (VE) and the June 9 at 23:33 GMT aftershock of the Victoria earthquake. SS = Salton Sea; SJF= San Jacinto Fault; BSZ = Brawley Seismic Zone; MSZ = Mexicali Seismic Zone; SHF = Sand Hills Fault; LSF = Laguna Salada Fault; SaJF = Sierra Juárez Fault; CR = Colorado River; CG = California Gulf. The segmented lines enclose the seismic zones (BSZ and MSZ) based on seismic activity (Johnson, 1979; Frez and González, 1987).

high-gain portable stations with analog (smoked paper) or digital recording. These stations are the same or similar to those previously used by Albores *et al.* (1980). Additional local data were obtained from stations NVL, QKP, SON, TLX and VER of the Seismological Network of Northwest of Mexico (RESNOM), operated by CICESE: one additional station (TRI) had only a limited use. The earlier aftershocks were located by the RESNOM stations five hours after the main shock. Digital data from the Southern California Seismological Network (SCSN), jointly operated by the U.S.Geological Survey (USGS) and the California Institute of Technology (Caltech), were not available for the events of June 1980 (Wald *et al.*, 1994). A few arrival times were taken from the Bulletin of the International Seismological Centre and from card records of USGS/Caltech, but our epicenter determinations depend almost exclusively on local data. Figure 1 shows the locations of local and regional stations used or mentioned in this study; additional information on these stations is given in Table 1. The temporary network operated for almost seven days until June 16, 1980. Other observations and studies are found in Frez (1982), Wong and Frez (1982), Suárez *et al.*, (1982), and Lesage and Frez (1990).

2. SURFACE EFFECTS

In this section we summarize surface and airborne reconnaissance observations by Suárez *et al.*, (1982), related to the main shock. The epicentral area lies in a zone of irrigated farms where no important engineering structures designed to withstand earthquakes exist, except the Cerro Prieto geothermal plant (Figure. 4).

A day and a half after the main event the Mexicali Valley was inspected by air, from the International Border to the head of the Gulf of California. Shallow cracks and fractures perpendicular, or near perpendicular, to the probable strike of the Cerro Prieto fault were identified. No consistent visible scarps were found on the fault line. Associated with the fractures were many sand blows and pits, especially near the fault trace between the Cerro Prieto geothermal field and the locality of Luis B. Sánchez (Figure 4).

Cobos (1980) mapped three sets of fractures, with NW-SE, NE-SW, E-W and random orientations. These fractures are not tectonically generated, and can be related to liquefaction. During a field trip, surface fractures up to 100 m long were found around water drains and the irrigation channels. In two places, near the trace of the Cerro Prieto fault, the fractures could be due to tectonic slippage. One site, on a road southeast the locality of Oaxaca, had many extensional transverse cracks, with about 2 cm right-lateral displacement. The other location, 2.5 km west of the Murguía railroad station, featured a 6 m wide zone of fracturing. Here the fractures were parallel to the trace of the Cerro Prieto fault and showed up to 1 cm right-lateral motion.

The most severe damage was observed in the small towns of Olachea and Pescaderos (Figure 5). Here 13 out of 39 adobe houses suffered major damage to complete destruction. Two out of 19 concrete block houses were severely damaged. Some irrigation channels were completely destroyed. Figure 5 shows that the area of maximum damage does not coincide with the area inmediately surrounding the epicenter; this can be explained by the absence of settlements.

Geodetic measurements by Lisowski and Prescott (1982) are consistent with right-lateral transform faulting striking N42°W for the Cerro Prieto fault; however, geodetic results on the Cerro Prieto fault near Mesa de Andrade suggest compression parallel to the trace of the fault during the time period which included the Victoria earthquake (Darby *et al.*, 1981).

The aftershocks migrated to the northwest, starting from the epicenter of the main event (Anderson *et al.*, 1982). This agrees with the direction of rupture propagation of the main shock (Lesage and Frez, 1990). Ground accelerations for Victoria (at an epicentral distance of 10 km) exceeded 1.0 g in the vertical and horizontal directions (Simons, 1982). Large accelerations may be due to a high stress drop at the source and/or large amplification of the ground motion due to a thick sedimentary cover (Munguía and Brune, 1984). Changes in ground elevation and gravity were observed locally; the increase in gravity indicates that subsidence took place east of the northwestern end of the Cerro Prieto fault (Zelwer and Grannell, 1982).

In conclusion, there is no clear evidence of fault rupture at the surface from this earthquake. The focal displacement at depth was damped at the surface by the thick sediment cover. Geodetic measurements indicate a strike-slip motion for this event (Lisowski and Prescott, 1982).

3. THE MAIN SHOCK

Twenty-four readings of P-wave arrivals, with epicentral distances between 30 km and 150 km, were used to locate the hypocenter of the main shock. The nearest station (30 km) was QKP. Ten strong-motion stations, operated jointly by UNAM and UCSD, yielded accelerograms for the main event (Anderson *et al.*, 1982; Simons, 1982); however, only one S-P time observation at Cucapah (CUC), was used in the hypocenter determination.

We locate the hypocenter at 32° 11' ± 3' N, 115° 03' ± 2' W, with a focal depth of 9 ± 4 km, and the origin time at 03:28:19.6 ± 0.7. The error estimations are based on the dispersion of different solutions rather than on the smaller errors given by HYPO71 (Lee and Lahr, 1975). In different numerical experiments, we varied the weighting factors associated with epicentral distances and the initial point for the iterative calculation; also we selected different station sets, for example, in the Mexicali-Imperial Valley only. The RMS values are generally small, reaching up to 0.12 when using only stations in and around the Valley. There is a trade-off between depth, origin time, and latitude. A shallower focus is associated with either a later origin time or a more northern latitude; for example, a latitude of 32° 12' is compatible with a depth of 6 km. Our location is near the SCC epicenter (32° 11.12' N; 115° 04.15' W). Our longitude estimation is quite stable different in numerical

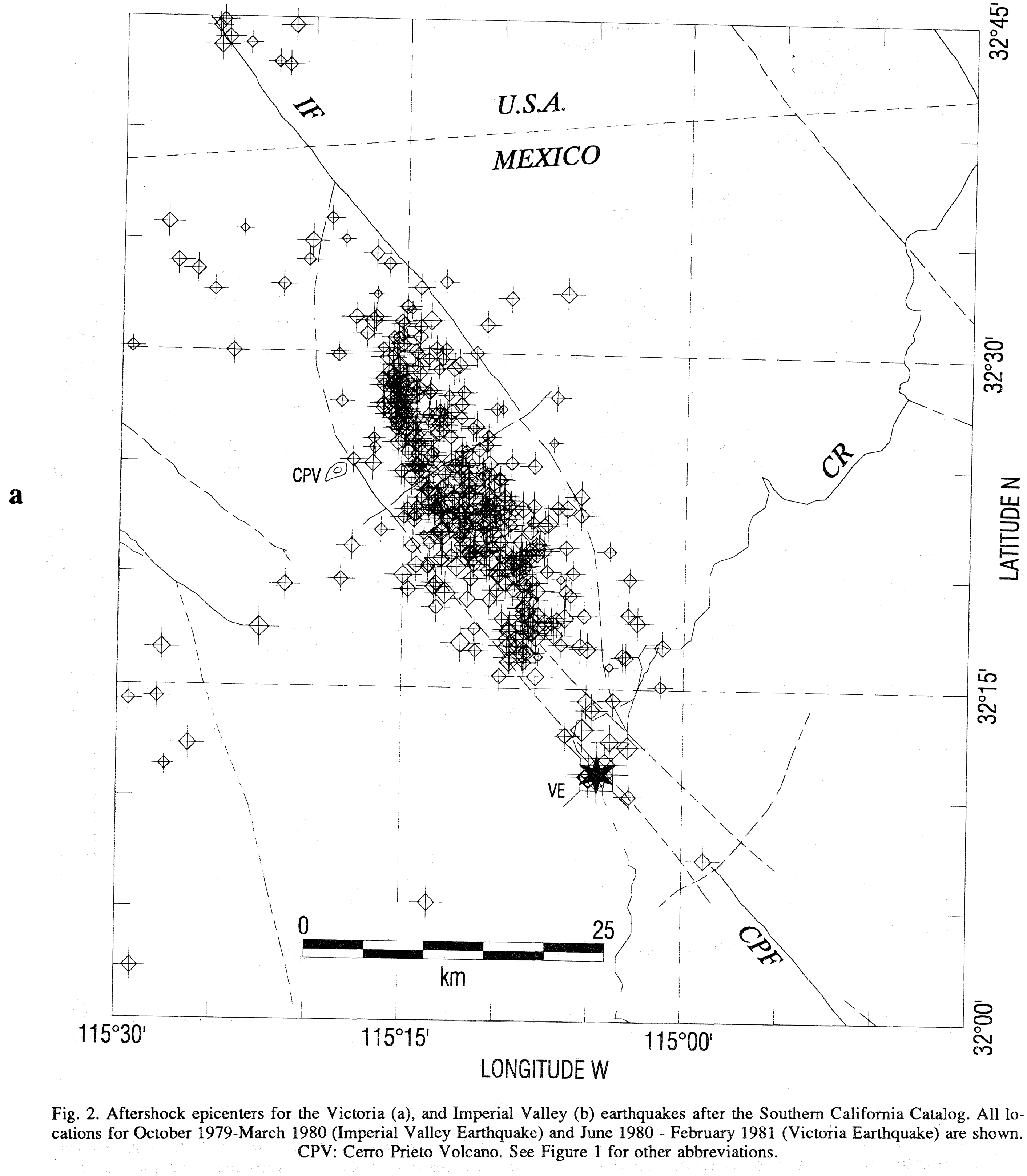

Fig. 2. Aftershock epicenters for the Victoria (a), and Imperial Valley (b) earthquakes after the Southern California Catalog. All locations for October 1979-March 1980 (Imperial Valley Earthquake) and June 1980 - February 1981 (Victoria Earthquake) are shown. CPV: Cerro Prieto Volcano. See Figure 1 for other abbreviations.

tests; it puts the epicenter closer to the Cerro Prieto fault. Both locations use practically the same stations.

The useful arrival times are distributed in an azimuthal range of only 90° around the estimated epicenter, which introduces instability in the hypocenter determination. In order to optimize the data resolution, we took several steps. First, we used corrections to the arrival times for each station. Second, we used a structure for the Mexicali Valley (Table 2) based on the model SP-6 (Fuis *et al.*, 1982) for the Imperial Valley. Third, we used the well-recorded aftershock of June 9, at 23:33 GMT ($M_L = 4.3$) as a calibration

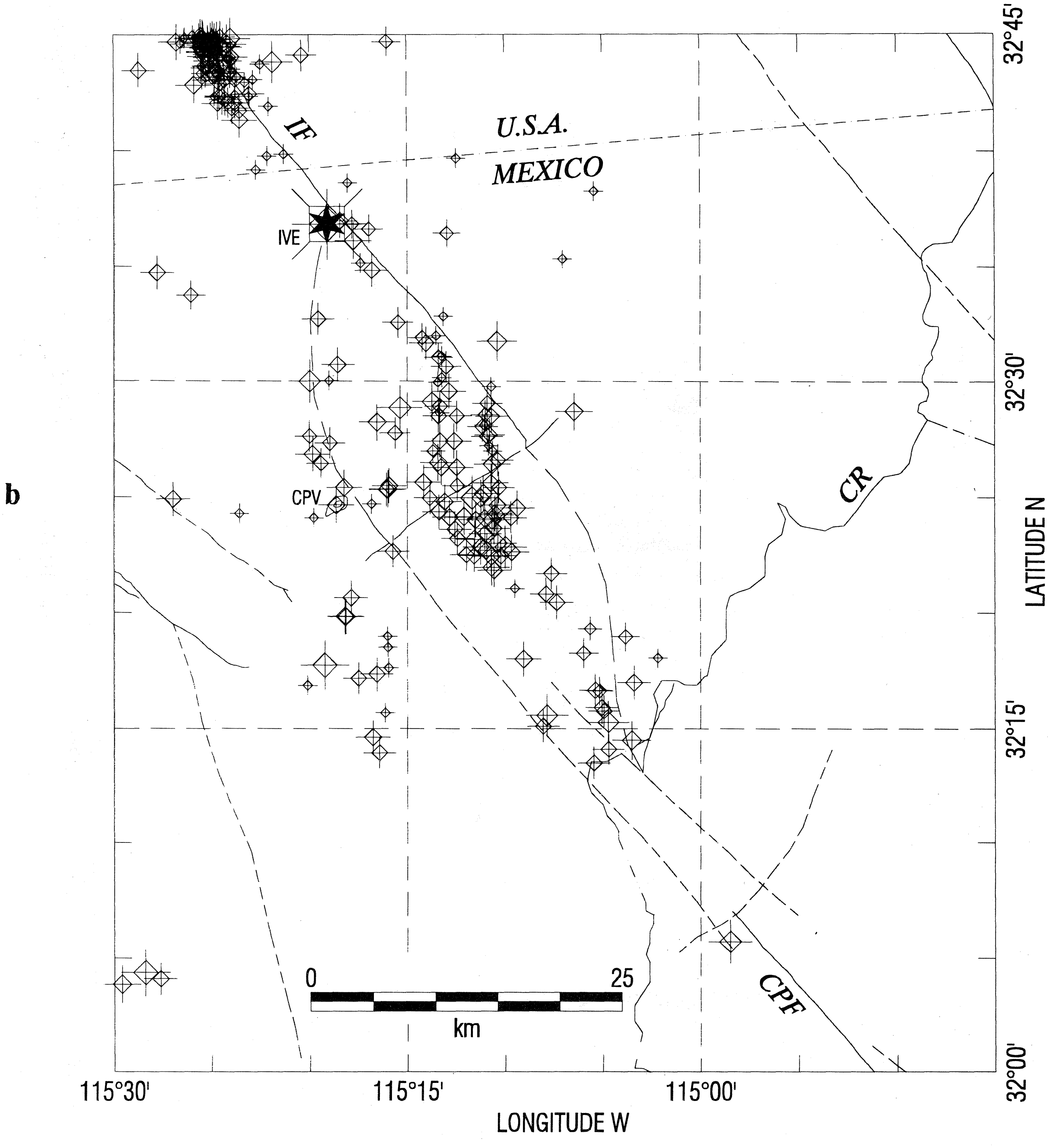

Fig. 2. (Cont).

event. In addition, we tested the stability of our calculations by selecting subsets from our data set. Finally, we analyzed our results in the context of the known features of Mexicali Valley seismicity (Frez and González, 1987; Frez and González, 1990).

The station corrections were obtained from the 17 best aftershocks located using local arrival times. Mean residuals were computed for each of the regional stations. The average azimuthal range in these determinations is about 100°. A similar approach was reported by Frez and González (1987). Arrival corrections consisted of:

(a) Small, mostly negative corrections for stations situated over sediments in the Valley, as at BON (-0.05), CLI (-0.03), VER (-0.02), NVL (-0.01).

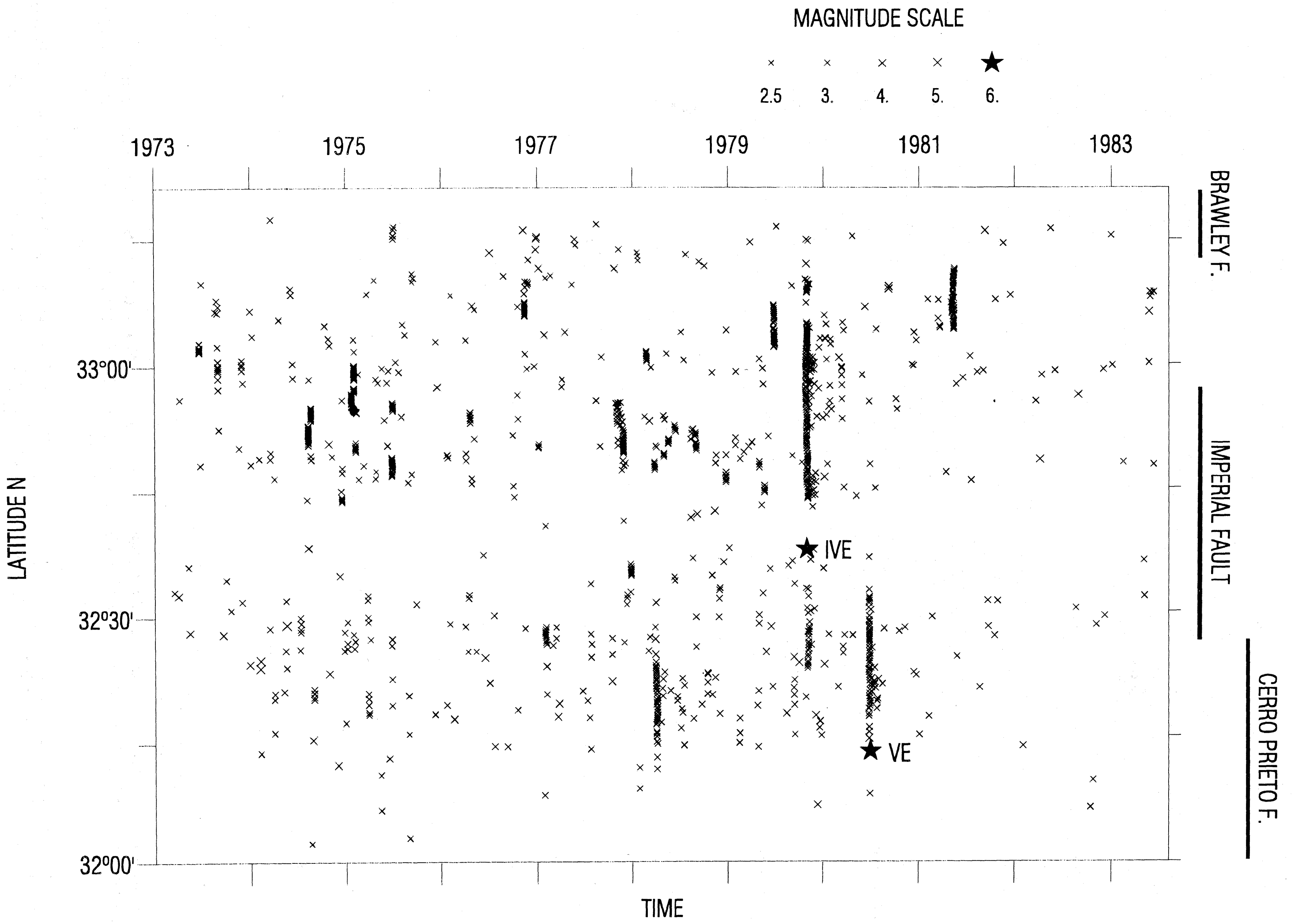

Fig. 3. Seismicity (M_L>2.5) of the Imperial-Mexicali Valley in time and latitude. The events are projected onto the average trend of the Imperial/Cerro Prieto Fault System. The latitudes correspond to the average position of the traces of both faults. The epicenters included in this Figure are inside a rectangular window of about 15 km width centered on the average position of the faults. Solid stars, main shocks of the Imperial Valley and Victoria earthquakes.

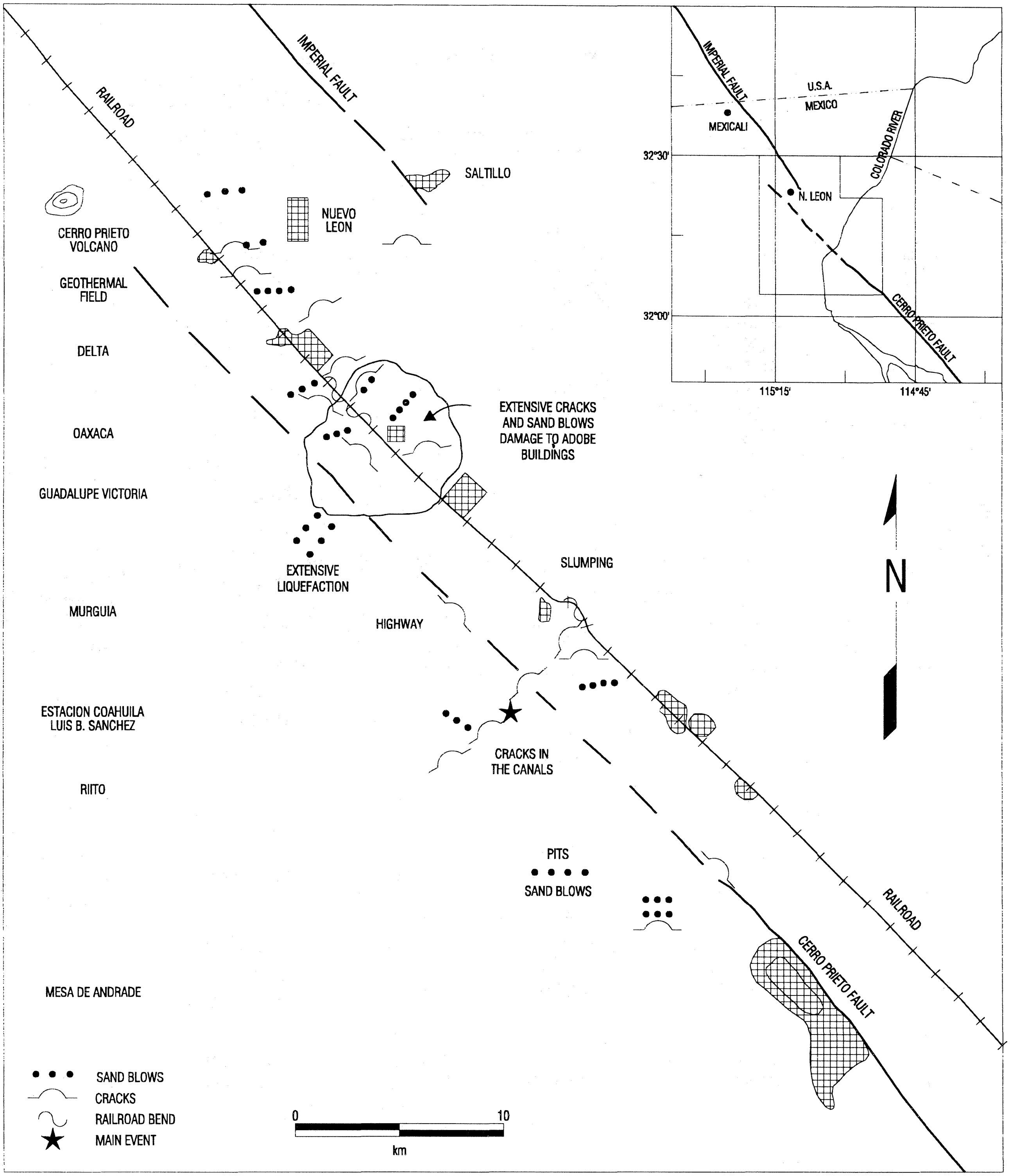

Fig. 4. Ground surface effects of the main shock from field observations. Names of the localities (crosshatched) are shown at left margin. The solid star represents the epicenter of the main shock.

(b) Small, mostly positive corrections west of the Valley and on granite, as for SGL (+0.07), ILP (+0.05), SUP (-0.04).

(c) Positive corrections for stations east of the Valley, as for PLT (0.17), YMD (0.10), RUN (0.19), GLA (0.11).

(d) Positive corrections near the Pacific coast in the Peninsular Ranges, as for BAR (0.34), PLM (0.45), and TRI (0.48).

The June 9 aftershock at 23:33 GMT (M_L = 4.3) was recorded by a significant number of both local (3) and regional (20) stations. With a range of 118° in azimuth, an

Table 1

Station parameters for Local and Regional Stations

STATION NAME	NETWORK	LATITUDE (N)	LONGITUDE (W)	OPERATION PERIOD day/hour	SITE GEOLOGY
AMS	SCSN	33° 08.48'	115° 15.25'	permanent	rock
BAR	SCSN	32° 40.80'	116° 40.30'	permanent	rock
BON	SCSN	32° 41.67'	115° 16.11'	permanent	sediments
BSC	SCSN	32° 43.49'	115° 02.64'	permanent	sediments
CH2	SCSN	33° 17.77'	115° 20.17'	permanent	rock
CLS	LOCAL A	32° 19.50'	115° 06.50'	10/20-15/19	sediments
COA	SCSN	32° 51.81'	115° 07.36'	permanent	sediments
COK	SCSN	32° 50.95'	115° 43.61'	permanent	rock
COL	LOCAL A	32° 08.58'	115° 08.15'	12/21-16/20	sediments
CRR	SCSN	32° 53.18'	115° 58.10'	permanent	rock
CUC	SMS	32° 32.72'	115° 14.08'	permanent	sediments
ELN	LOCAL A	31° 50.58'	115° 09.80'	10/16-11/19	rock
FRO	LOCAL A	32° 16.37'	115° 17.88'	10/22-16/22	rock
GLA	SCSN	33° 03.10'	114° 49.60'	permanent	rock
IKP	SCSN	32° 38.93'	116° 06.48'	permanent	rock
ING	SCSN	32° 59.30'	115° 18.61'	permanent	sediments
JR	LOCAL D	32° 07.80'	114° 57.85'	9/20-16/12	sediments
NVL	RESNOM	32° 23.91'	115° 12.66'	permanent	sediments
NW2	SCSN	33° 05.43'	115° 41.54'	permanent	sediments
OLA	LOCAL D	32° 20.25'	115° 09.83'	9/20-13/23	sediments
PLM	SCSN	33° 21.20'	116° 51.70'	permanent	rock
PLT	SCSN	32° 43.87'	114° 43.76'	permanent	sediments
QKP	RESNOM	32° 18.30'	115° 19.92'	permanent	rock
RD	LOCAL D	32° 12.45'	114° 58.80'	11/22-16/14	sediments
RHA	LOCAL D	32° 08.10'	115° 17.07'	9/20-16/12	rock
RUN	SCSN	32° 58.33'	114° 58.63'	permanent	sediments
SAL	LOCAL A	32° 25.60'	117° 22.50'	11/18-15/2	sediments
SGL	SCSN	32° 38.95'	115° 43.52'	permanent	rock
SNR	SCSN	32° 51.71'	115° 26.21'	permanent	sediments
SON	RESNOM	32° 17.50'	115° 09.83'	permanent	sediments
SUP	SCSN	32° 57.31'	115° 49.43'	permanent	rock
TLX	RESNOM	32° 29.39'	115° 08.71'	permanent	sediments
TRI	RESNOM	31° 52.97'	116° 39.87'	permanent	rock
TYL	LOCAL A	32° 14.00'	114° 58.50'	9/22-15/18	sediments
UVA	LOCAL D	32° 15.00'	115° 05.94'	9/24-14/3	sediments
VER	RESNOM	32° 21.67'	115° 06.32'	permanent	sediments
VIC	SMS	32° 17.40'	115° 06.00'	permanent	sediments
WIS	SCSN	33° 16.56'	115° 35.58'	permanent	sediments
WLK	SCSN	33° 03.08'	115° 29.44'	permanent	sediments
YMD	SCSN	32° 33.28'	114° 32.68'	permanent	sediments

SCSN:	Southern California Seismological Network.
RESNOM:	Seismological Network of Norwest of Mexico.
LOCAL:	Temporal, local network (A: analog, D: digital).
SMS:	Strong-motion station.

RMS value of 0.16, and a nearest observation (NVL) at 7.4 km, this hypocenter was better located than the main shock (Table 3). We calculated differences in arrival times for both events at 19 stations. The YMD station is located at midway latitudes between the main event and the aftershock (see Figure 1); the difference in computed travel times based on our location is only 0.3 s. The distribution of the differences in arrival times, assuming a value of 0.0

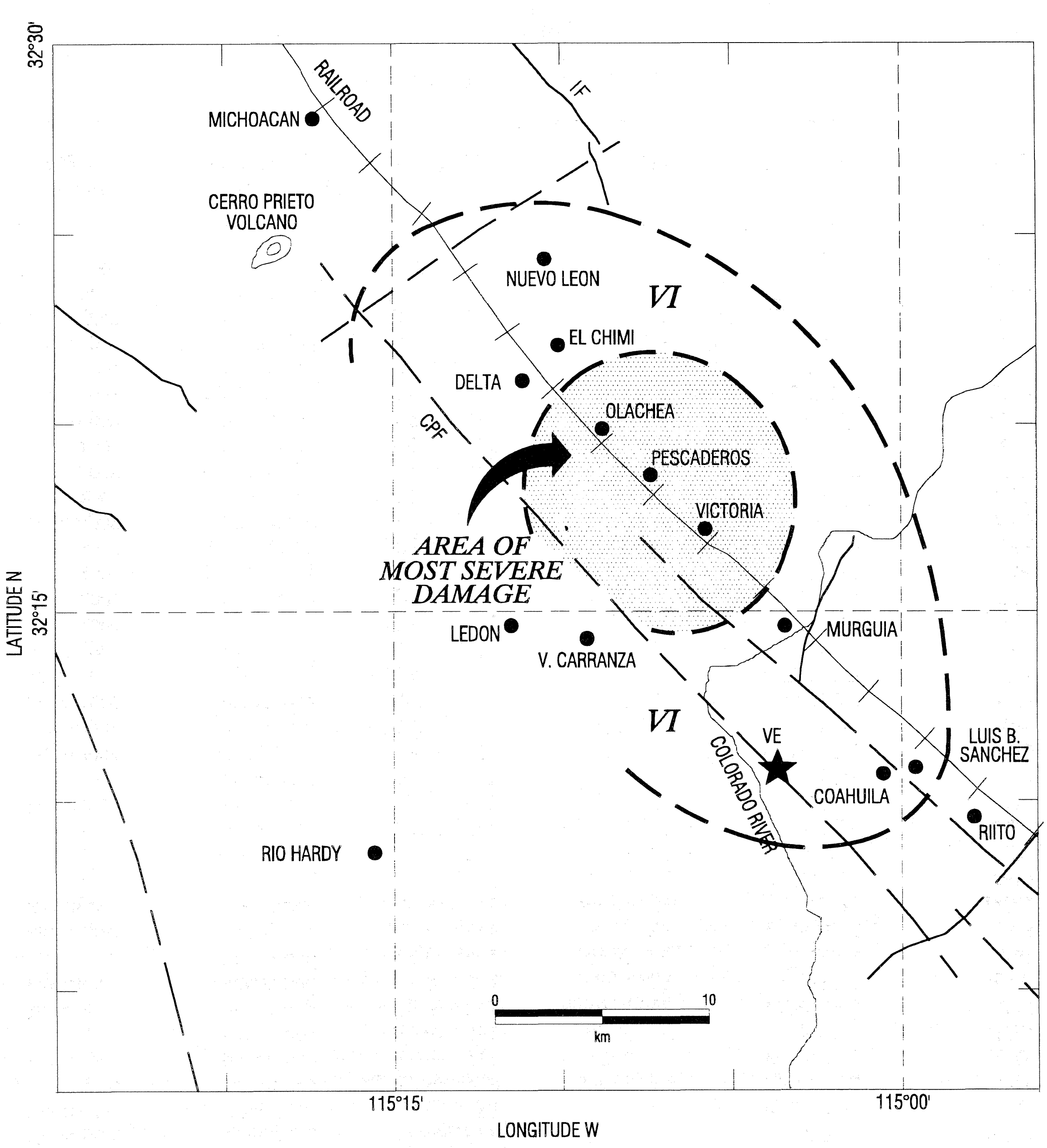

Fig. 5. Area of damage corresponding to a modified Mercalli Intensity of VI. The solid star shows the location of the main shock. VE: Victoria Earthquake; CPF: Cerro Prieto Fault; IF: Imperial Fault. The area of most severe damage correspond to the extensive ground cracking, sand blows and damage to adobe houses.

for YMD station, gives a systematic pattern with differences of up to 3.5 s to 3.7 s for stations located at azimuths of 270°-360°. A main shock located 18 km SE and 8 km deeper than the aftershock fits this pattern, using a horizontal Vp velocity of 6.0 km/s, an average vertical velocity of 5.0 km/s and an incidence angle of 50° to 65°.

The nearest station to the main shock (QKP) had an epicentral distance of 30 km; thus the focal depth is not well resolved. However, the proposed depth of 9 ± 4 km is reasonable, since our determinations yield depths of 6-15 km on the basis of a realistic structure for the Mexicali-Imperial Valley, where the stations with the smaller time corrections are located. This lend more weight to the calculations associated with, indirect, diving, refracted rays. As we shall see, aftershocks depths increase to the SE along the Cerro Prieto fault, which agree with a value of 9 km for the focal depth. Southern California and northern Baja California earthquakes of $M \geq 6.0$ are generally located at the bottom of seismogenic zone, though this was not true of the Landers earthquake of June 28,1992.

The main shock was located at the SE end of the aftershock region which is compatible with an unilateral rup–

Table 2

Crustal Velocity Model

Layer	P-wave velocity* (km/s)	S-wave velocity** (km/s)	Depth to the top of the layer (km)
1	2.000	0.800	0.000
2	2.533	1.055	0.500
3	2.900	1.261	1.250
4	3.267	1.485	1.750
5	3.633	1.730	2.250
6	4.000	1.905	2.750
7	4.367	2.184	3.250
8	4.773	2.367	3.750
9	5.100	2.684	4.250
10	5.375	2.986	4.750
11	5.650	3.139	5.250
12	5.750	3.194	5.750
13	5.800	3.222	6.750
14	5.850	3.250	7.600
15	6.600	3.708	7.900
16	6.800	3.820	8.200
17	7.000	3.933	8.500
18	7.200	4.045	12.500
19	7.500	4.289	17.000
20	7.800	4.457	20.000

*Based on Fuis *et al.* (1982).
**Based on González *et al.* (1983).

ture towards the NW end of the Cerro Prieto fault as found by Lesage and Frez (1990), and Anderson *et al.* (1982). This location is at the SE end of the Mexicali Seismic Zone. Similarly, the Imperial Valley and El Centro earthquakes were at the north end of the Mexicali Seismic Zone (Imperial Fault) and the SE end of the Brawley Seismic Zone, respectively (Johnson, 1979; Frez and González, 1987). Aftershocks of these main events were mostly located inside the Mexicali and Brawley seismic zones.

We used 133 teleseismic first motions of P-waves to obtain a well constrained solution of the focal mechanism. We obtain a vertical fault with a strike of 315° and right-lateral motion (Figure 6). Inconsistencies are found for the following stations: AAG, SNA, KHE, COM, COK, AN1, AN2, AN3. This improves our previous solution (Frez, 1982) and agrees with the results of Nakanishi and Kanamori (1982). An analysis of teleseismic waveforms (Lesage and Frez, 1990) is also consistent with the present solution; the latter study gives estimates of the rupture velocity (0.90 of the S-velocity), the displacement dislocation (0.60 m), and suggests a complex rupture process with an unilateral fracture propagating to the NW.

The question of possible foreshocks is complicated by inadequate information on background seismicity. However, records from two stations (QKP and NVL) indicate that two minor swarms occurred just before the main shock. From S-P arrival times, we found that these swarms occurred at the southern region of the aftershock area. The first swarm consisted of 15 events and occurred 19 hours before the main event; a shock with a maximum local magnitude of 3.0 was located about 2 km north of the main shock according to the SCC. The second swarm consisted of 4 events, one hour before the main event; it had a maximum local magnitude of 1.0. Note that no foreshocks were identified before the October 15, 1979, Imperial Valley earthquake (Johnson and Hutton, 1982).

4. AFTERSHOCK LOCATIONS AND FAULT MECHANISMS

Both P and S phases were used in locating the aftershocks using at least five recording stations. Values of S-velocities (Table 3) were obtained from the P-velocities by using reported values for the Vp/Vs ratio within the sediments of the Mexicali Valley (González *et al.*, 1983; Frez y González, 1990). The average Vp/Vs ratio is 2.2; below the sediments, this ratio is estimated as 1.78. These values are consistent with results for Imperial Valley (Archuleta, 1982, Nicholson and Simpson, 1985). First arrivals for S-waves are sometimes difficult to identify because of a large-amplitude late arrival which can be confused with a true S-phase. This phase has been interpreted as the first of

Table 3

Aftershock Parameters

Earthq. No.	Date (y/m/d)	Origin Time (GMT)	Latitude	Longitude	Depth (km)	Mag	NO	GAP	DMIN	RMS	ERH	ERZ	S/D
1	800609	08:02:03.39	32° 21.52'	115° 13.83'	6.53	2.0	7	144	4.8	.02	.2	.4	A/C
2	800609	08:11:00.03	32° 23.05'	115° 16.22'	7.44	2.0	6	197	5.8	.06	1.0	.4	A/D
3	800609	08:26:03.37	32° 22.00'	115° 13.97'	7.05	2.7	6	156	4.1	.07	.7	1.8	A/C
4	800609	08:40:01.50	32° 20.09'	115° 13.55'	4.80	2.0	5	122	7.2	.01	.1	.4	A/D
5	800609	09:12:00.79	32° 22.05'	115° 13.98'	6.35	2.5	5	158	4.0	.06	1.0	2.0	A/D
6	800609	09:20:00.61	32° 25.88'	115° 16.35'	5.50	2.4	6	227	6.8	.04	.6	1.2	A/D
7	800609	09:45:08.01	32° 24.01'	115° 15.43'	6.55	2.2	5	199	4.3	.02	.4	.5	A/D
8	800609	10:12:08.05	32° 20.15'	115° 14.05'	4.26	2.0	6	128	7.3	.02	.2	.3	A/B
9	800609	10:45:59.85	32° 15.68'	115° 10.69'	6.04	3.2	5	257	3.6	.02	.8	.3	A/D
10	800609	19:48:10.25	32° 21.07'	115° 13.40'	5.10	3.2	5	129	5.4	.10	1.0	2.2	B/D
11	800609	23:33:39.70	32° 19.96'	115° 12.20'	1.00	4.3	24	108	7.3	.16	.5	1.8	B/B
12	800610	00:36:49.89	32° 21.76'	115° 10.07'	3.41	3.4	6	119	5.7	.06	.5	.8	A/B
13	800610	01:57:01.88	32° 20.21'	115° 12.97'	4.17	2.6	6	117	6.9	.05	.3	1.1	A/B
14	800610	02:09:37.72	32° 21.44'	115° 12.94'	7.43	2.5	10	124	4.6	.07	.4	.4	A/B
15	800610	02:36:36.53	32° 23.58'	115° 15.55'	3.45	2.7	5	195	4.6	.05	.7	.6	A/D
16	800610	03:41:00.44	32° 20.69'	115° 11.80'	5.02	3.4	8	99	6.1	.07	.3	.6	A/B
17	800610	03:48:44.04	32° 20.13'	115° 13.06'	7.35	2.8	6	132	5.5	.08	1.1	.9	B/B
18	800610	04:34:26/61	32° 19.82'	115° 11.44'	5.42	2.1	6	109	5.0	.02	.2	.3	B/B
19	800610	05:36:23.57	32° 22.29'	115° 13.68'	6.44	3.3	8	155	3.4	.05	.4	.7	A/C
20	800610	06:16:00.19	32° 17.60'	115° 11.92'	7.45	2.0	6	183	3.3	.05	.6	.6	A/D
21	800610	06:32:05.31	32° 24.01'	115° 13.66'	5.66	2.0	5	181	1.6	.03	.5	.4	A/D
22	800610	06:34:58.42	32° 26.68'	115° 15.44'	5.90	2.3	7	229	6.7	.03	.3	.3	A/D
23	800610	06:45:42.01	32° 22.54'	115° 11.61'	5.56	2.0	5	134	3.0	.01	.3	.4	A/D
24	800610	06:50:08.25	32° 22.11'	115° 12.43'	5.66	2.2	6	216	5.9	.07	1.2	1.7	A/D
25	800610	07:02:25.30	32° 22.82'	115° 11.26'	5.97	3.2	6	153	3.0	.03	.4	.6	A/C
26	800610	08:20:06.11	32° 21.11'	115° 11.44'	5.04	2.2	7	103	3.6	.06	.4	.7	A/B
27	800610	08:23:41.16	32° 23.62'	115° 13.00'	4.55	2.8	8	178	.8	.06	.9	.5	A/C
28	800610	21:42:07.56	32° 18.89'	115° 12.72'	4.99	2.2	6	181	5.4	.04	.4	.6	A/D
29	800611	00:13:35.97	32° 22.72'	115° 11.45'	4.24	2.0	5	107	2.9	.08	.8	.6	A/D
30	800611	01:12:39.08	32° 16.53'	115° 08.41'	5.88	2.8	9	132	2.9	.04	.3	.3	A/B
31	800611	03:36:23.04	32° 18.83'	115° 09.93'	6.88	2.0	12	74	2.3	.08	.4	.4	A/A
32	800611	04:22:53.99	32° 14.07'	115° 06.43'	4.94	2.0	6	156	8.3	.03	.3	.5	A/C
33	800611	05:38:42.96	32° 22.31'	115° 12.85'	5.96	2.4	9	129	3.0	.05	.5	.6	A/B
34	800611	06:25:51.91	32° 21.03'	115° 11.68'	6.10	2.4	6	193	7.1	.02	.3	.4	A/D
35	800611	09:24:33.68	32° 18.70'	115° 09.44'	6.37	2.4	7	78	2.3	.03	.3	.3	A/A
36	800611	09:52:51.49	32° 23.28'	115° 12.57'	5.49	2.1	8	122	1.2	.05	.6	.6	A/B
37	800611	11:51:59.61	32° 17.60'	115° 10.88'	6.43	2.5	7	149	1.7	.05	.6	.4	A/C
38	800611	12:59:06.45	32° 16.28'	115° 08.38'	6.81	2.0	6	165	3.2	.04	.5	.5	A/C
39	800611	13:10:08.63	32° 27.07'	115° 14.63'	3.80	3.1	8	148	6.6	.05	.3	.5	A/B
40	800611	13:26:19.28	32° 16.26'	115° 11.54'	5.20	3.5	7	108	3.5	.03	.2	.3	A/B

Table 3 (Cont).

Earthq. No.	Date (y/m/d)	Origin Time (GMT)	Latitude	Longitude	Depth (km)	Mag	NO	GAP	DMIN	RMS	ERH	ERZ	S/D
41	800612	03:40:44.35	32° 15.40'	115° 09.36'	7.92	2.0	7	179	3.9	.10	1.2	1.0	B/C
42	800612	05:33:37.29	32° 16.19'	115° 08.45'	6.44	2.1	7	166	3.2	.04	.3	.4	A/C
43	800612	07:55:46.20	32° 14.32'	115° 08.05'	4.48	2.0	6	199	6.5	.05	.5	.6	A/D
44	800612	08:01:25.07	32° 16.21'	115° 08.84'	7.05	2.3	9	167	2.9	.04	.3	.3	A/C
45	800612	10:18:25.88	32° 20.82'	115° 11.21'	5.57	2.0	5	140	6.5	.02	.0	.2	A/D
46	800612	11:14:22.55	32° 16.51'	115° 09.54'	6.09	2.2	8	163	1.9	.09	.6	.8	A/C
47	800612	12:31:03.08	32° 23.00'	115° 10.92'	4.74	2.6	10	107	3.2	.06	.3	.4	A/B
48	800612	20:32:47.22	32° 27.78'	115° 12.48'	3.03	2.9	10	226	6.0	.09	.7	1.0	A/D
49	800612	23:59:10.75	32° 15.85'	115° 09.53'	6.76	2.9	11	102	3.1	.08	.4	.5	A/B
50	800613	08:05:33.97	32° 21.21'	115° 13.83'	5.41	2.2	11	139	5.3	.05	.3	.7	A/C
51	800613	08:11:56.79	32° 16.97'	115° 10.10'	6.37	2.0	8	93	1.1	.08	.5	.6	A/B
52	800613	08:14:28.45	32° 25.65'	115° 13.52'	4.83	2.9	9	241	3.5	.07	.7	.4	B/D
53	800613	13:12:40.92	32° 24.01'	115° 12.89'	5.03	2.2	9	209	.4	.09	.8	.6	B/D
54	800613	15:56:47.74	32° 17.25'	115° 06.85'	5.95	2.9	9	110	4.1	.02	.1	.2	A/B
55	800614	03:30:28.29	32° 16.78'	115° 10.35'	7.46	2.9	9	103	1.6	.05	.4	.3	A/B
56	800614	09:12:36.40	32° 20.29'	115° 14.21'	5.64	2.0	6	132	7.1	.07	.7	1.2	A/B
57	800614	10:36:04.34	32° 25.20'	115° 15.20'	4.70	2.3	5	241	4.6	.01	.4	.2	A/D
58	800614	16:28:48.30	32° 16.47'	115° 10.63'	5.44	2.8	8	107	2.3	.05	.4	.4	A/B
59	800615	03:27:29.37	32° 22.13'	115° 12.11'	6.45	2.0	6	110	3.4	.03	.5	1.1	A/D
60	800615	04:00:22.16	32° 16.72'	115° 08.81'	7.82	2.0	5	155	2.2	.06	1.3	.7	B/D
61	800615	09:09:04.89	32° 23.34'	115° 14.48'	4.61	2.0	7	207	3.0	.04	.9	.7	A/D
62	800615	16:02:07.46	32° 17.26'	115° 08.38'	7.07	2.0	5	128	4.8	.03	1.4	1.4	B/D
63	800615	16:14:51.73	32° 22.59'	115° 12.32'	5.12	2.0	5	113	2.5	.03	.7	.8	A/D
64	800616	00:14:22.54	32° 20.61'	115° 12.85'	7.34	3.1	5	114	6.1	.01	.1	.2	A/D
65	800616	00:14:48.84	32° 20.52'	115° 15.06'	5.48	3.1	5	149	7.3	.01	.1	.4	A/D

Mag: Local magnitude estimate based on CalTech-USGS Bulletin.
GAP: Largest azimuthal separation in degrees between stations as viewed from the epicenter.
RMS: Root mean square errors of travel-time residuals.
ERZ: Standar error of the depth.

NO: Number of Observations (P and S) used to compute hypocentral solution.
DMIN: Distance to closest seismograph station.
ERH: Standar error of the epicenter.
S/D: Reliability of hypocentral locations; where S is solution quality defined by HYPO71:

S	RMS	ERH	ERZ
A	< 0.15	< / = 1.0	< / = 2.0
B	< 0.30	< / = 2.5	< / = 5.0
C	< 0.50	< / = 5.0	< / = 7.50
D	others		

and D is station distribution quality defined by HYPO71:

D	NO	GAP	DMIN
A	> / = 6	< / = 90	< / = DEPTH or 5 km
B	> / = 6	< / = 135	< / = 2(DEPTH) or 10 km
C	> / = 6	< / = 180	< / = 50 km
D	others		

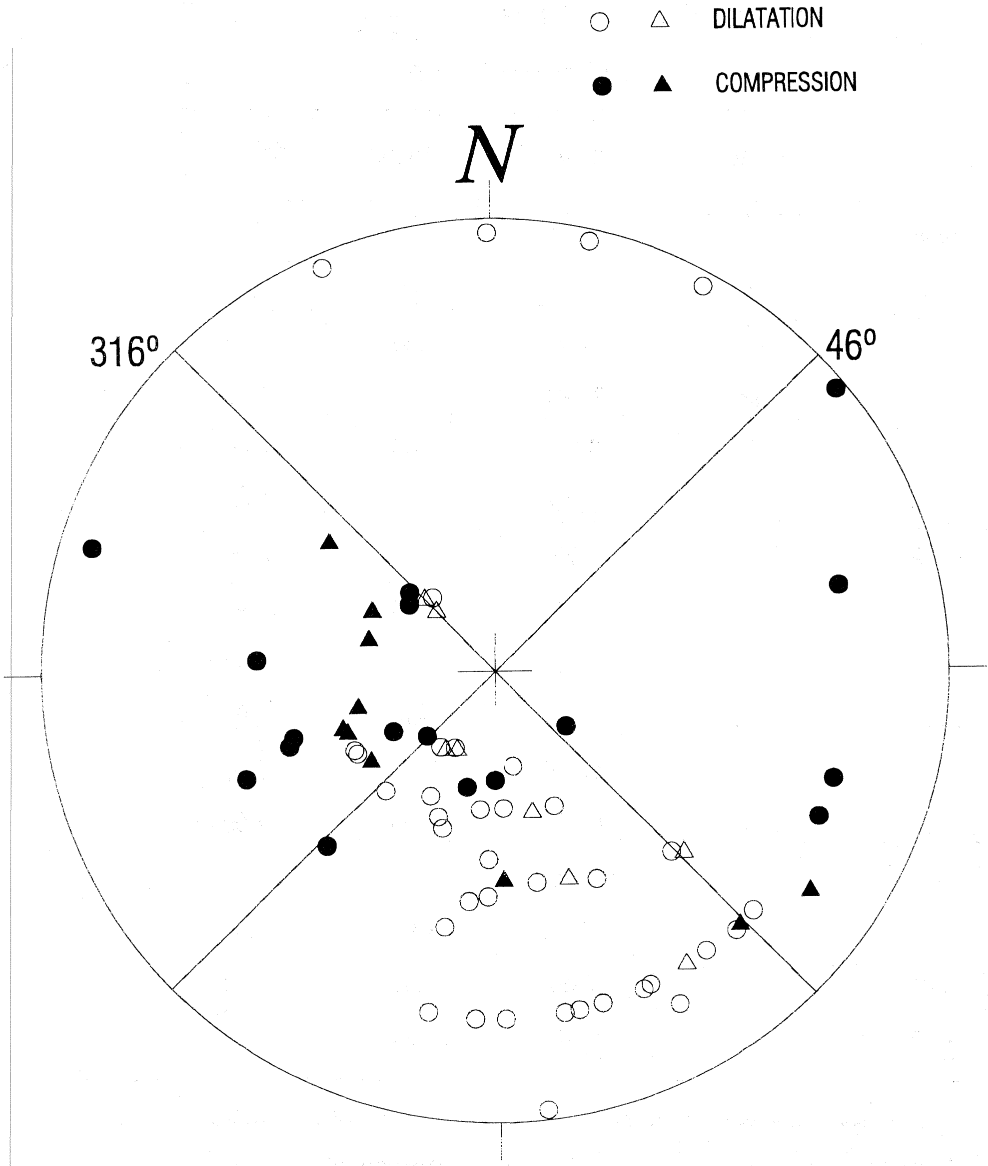

Fig. 6. Equal-area projection of the fault-plane solution for the main shock (upper hemisphere). Solid symbols, compression; open symbols, dilatation. Triangles correspond to small-amplitude or uncertain observations.

several multiple P-arrivals, excited by diffraction from beneath the base of the sedimentary layer (Frez *et al.*, 1983; Frez y González, 1990; Mori, 1992).

We used a modified version of HYPO71 which allows variations of the Vp/Vs ratio as a function of depth. This improves significantly the determinations, as true S-wave arrivals are additionally taken into account. S-wave arrival times were obtained from horizontal-component seismograms or from stations with epicenter distances less than 10 km. Arrival-time reading errors are between 0.05 s and 0.10 s for P-waves; the smaller errors correspond to digital records. Errors for the S-wave arrivals are two to three times larger. Among the 65 aftershock epicenters (Table 3), 27 were obtained with the P-wave arrivals only; the rest had contributions of one (27), two (13) and three (3) S-wave arrivals. Thus the hypocenters were mainly determined from P-wave arrival times.

The station distribution was nearly uniform in azimuth; with one exception, all solutions had at least one observation at a distance of less than 7.5 km. The maximum epicentral distance was generally between 15 and 25 km; thus nearly all first-arrivals were directed upward from the hypocenter, and locations are independent from the deeper structure. P-wave time corrections of -0.15 s and -0.10 s were found for the stations QKP and FRO, but all other stations on the Mexicali Valley sediments had zero correction. The station delays for QKP and FRO were found by trial and error.

Typically, the program HYPO71 converged in five iterations. True errors are probably less than 2 minutes in latitude and longitude and less than 3 km in depth. We made some numerical experiments with different structures and initial points. The solutions changed by up to 3 km horizontally or in depth, but the relative position of the

Table 4

Traveltime Residuals

Station Name	NRES	SRWT	AVRES	SDRES	NSARRIV
BON	1	1.67	.00	.00	---
CLS	30	26.47	.00	.06	13
COL	11	14.42	.00	.05	---
FRO	18	22.81	.03	.03	---
JR	6	3.71	.04	.06	2
NVL	50	68.28	.00	.04	23
OLA	9	6.23	-.03	.09	5
QKP	64	99.78	.00	.02	6
RD	3	1.93	.05	.11	---
RHA	1	1.46	-.03	.00	---
SAL	15	15.26	-.01	.07	2
SON	61	69.79	.00	.05	2
TLX	25	20.65	.02	.06	2
TYL	40	25.93	.01	.07	2
UVA	3	2.06	.01	.10	---
VER	57	56.44	-.02	.04	7

NRES: Number of residuals

AVRES: Average of residuals

SRWT: Weighted sum of residuals

SDRES: Standard deviation of residuals

NSARRIV: Number of S-wave arrivaltimes

hypocenters was stable. Table 4 gives the residual statistics from one set of locations. The standard deviations remained around 0.10.

The aftershocks cluster in two different regions. One cluster of aftershocks is close to the trace of the Cerro Prieto fault (A in Figure 7). The other cluster is towards the northwest (B, Figure 7). Some aftershocks (labeled C) scatter between the northwest end of the Cerro Prieto fault and the southeast end of the Imperial fault. There is a gap between the location of the main event and the aftershock epicenters. Independent hypocenter determinations from the SCC catalog show a similar gap; however, the SCC also shows nine epicenters at distances less than 10 km from the main shock epicenter. Eight of them occurred within three and a half hours of the main shock. These locations are shown in Figure 8, but not in Figure 7.

The aftershocks follow the general pattern of seismicity of the Mexicali-Imperial Valley (Johnson and Hill, 1982; Frez and González, 1987). The aftershock distribution in Figure 4 resembles earlier microseismicity studies in the region (Albores *et al.*, 1980). The Southern California Catalog contains about 355 epicenters which can be taken as aftershocks of the Victoria earthquake up to August, 1980; of these, 210 belong to a subset with $M_L \geq 2.2$ which may be assumed to be complete. The threshold of 2.2 is found from the magnitude statistics. The b-value is 0.96 ± 0.15 by the maximum likehood method. Kisslinger and Jones (1991) found a b-value of 1.05 ± 0.37 using a minimum magnitude of 3.0; in addition, they found a p-value of 1.52 ± 0.19 for the Omori relation.

Epicenter determinations from USGS/Caltech have systematic differences with our locations. Southern California

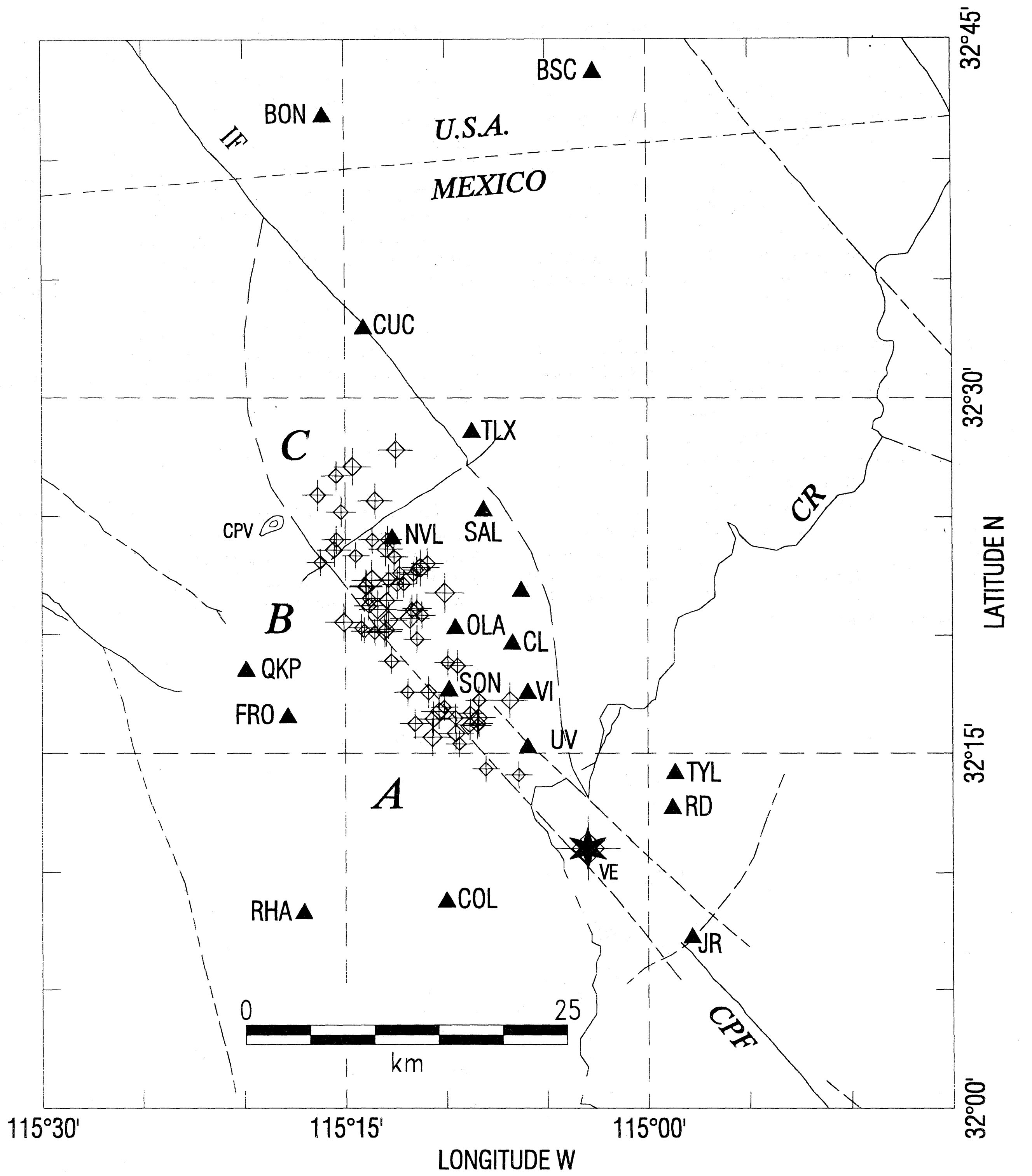

Fig. 7. Local seismological stations used in this study (open triangles); epicenter of the main event (solid star); and aftershocks. A, B, and C regions of aftershocks mentioned in the text. Only aftershocks located in this study are included. VE: Victoria Earthquake; IF: Imperial Fault; CPF: Cerro Prieto Fault.

Catalog place the epicenters about 3.5 km to the north. For example, our determination for the aftershock of June 9 at 23:33 GMT is almost 2' to the south and 0.5' to the east of the location given by USGS/Caltech. Frez and González (1990) reported a systematic error of opposite sense for the Imperial Valley aftershocks located near the Imperial fault, south of the International Border. This difference might be due to a lower seismic velocity associated with the Mexicali Seismic Zone and/or a systematic error in the USGS/Caltech locations due to azimuthal coverage.

A section along the strike of the Cerro Prieto fault (Figure 8a) suggests that the clusters of aftershock activity are at different depths; the aftershocks becoming on average deeper southward from the end of the fault. While our locations are structure dependent, numerical experiments suggest that the general trend shown in Figure 8a. is stable. The aftershock sequence of the Imperial Valley earthquake of October 15, 1979 indicates a similar behaviour, i.e., a decrease in the depth of the aftershocks at the southeast end of the Imperial fault (Frez and González, 1987). A cross-section perpendicular to the strike of the fault (Figure 8b) shows that the activity concentrates between 4 to 6 km towards the center of the seismic zone.

Figure 8c shows the position of the epicenters in time. We started to locate aftershocks five hours after the occurrence of the main shock. Epicenter determinations taken from the SCC catalog partially fill the gap by locating 32 aftershocks in the first five hours. Four of these aftershocks are estimated to be very close to the main event; the others are in the regions of high seismicity defined above. Depth determinations from the SCC catalog have systematic errors (Figure 8a and 8b). Figure 8c shows epicenter migration; the activity propagated in an approximately uniform way with some reduced activity in region A (i.e., nearest to the main shock location) during the forty hours following the main shock.

Composite focal mechanisms for clusters A and B are shown in Figures 9a and 9b. A vertical strike-slip fault is associated with the southeastern cluster found near Cerro Prieto fault, whereas the activity situated towards the northwest is produced by normal faulting. The earthquake cluster at the northern end of the aftershock area (C in Figure 7) suggests a normal dip-slip solution, but there is not enough information to produce a precise determination. The direction of the nodal planes and the maximum tensile axis are consistent with other solutions and with the tectonic interpretation for this region (Lomnitz *et al.*, 1970; Elders *et al.*, 1972; Weaver and Hill, 1978). These authors considered a tectonic system of transform faults joined by spreading centers, where near-horizontal tensional stresses are predominant. Other focal mechanisms in the Mexicali-Imperial Valley are discussed elsewhere (Frez and González, 1987).

5. DISCUSSION AND CONCLUSIONS

The Victoria earthquake is related to an increase in seismic activity observed in the Mexicali-Imperial Valley during 1973 to 1981 (Johnson and Hill, 1982; Frez and González, 1987). This activity consisted of many earthquake swarms and included the Imperial Valley earthquake of October 15, 1979 .

a

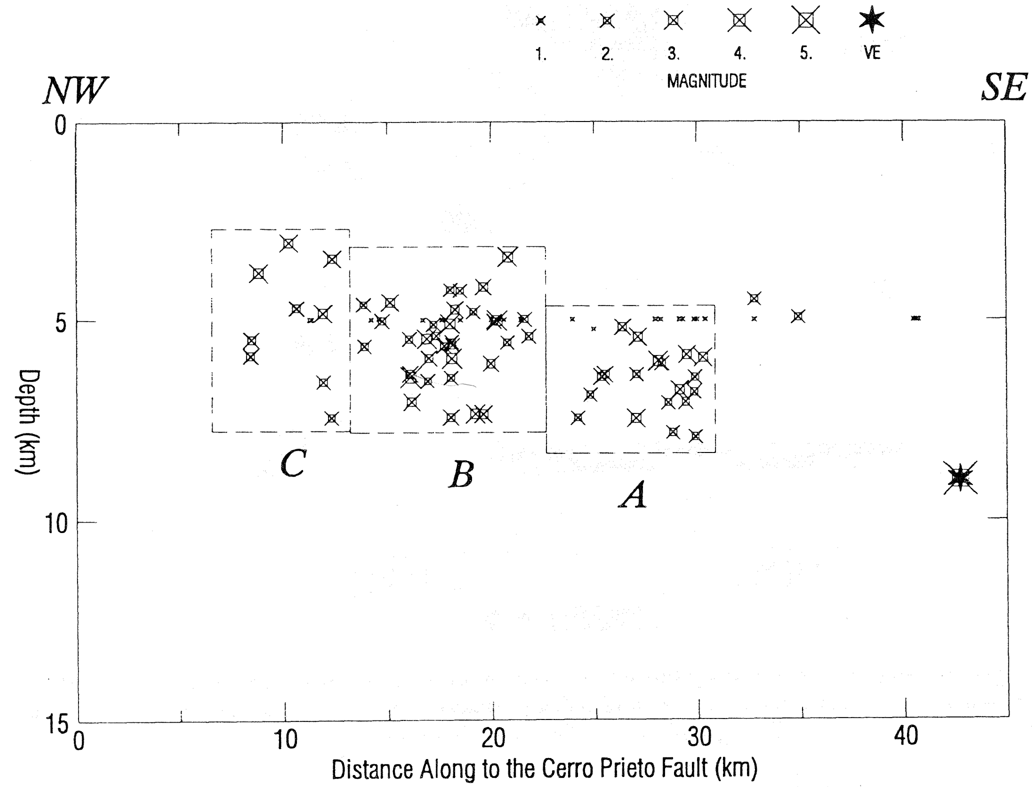

Fig. 8. Main shock (solid star) and aftershock distribution in time and space. Small asterisks correspond to locations taken from the Southern California Catalog in the first twenty-four hours after the main shock. Normal-size symbols represent epicenters of aftershocks located in this study.
(a) Section along fault strike showing locations of earthquakes used in Figure 7. Reference point at: 32° 25' N and 115° 25' W.
(b) Cross-section normal to the fault strike showing locations of hypocenters used in Figures 7 and 8 (a).
(c) Time-space distribution of the earthquake data used in Figures 7, 8 (a) and 8 (b). The horizontal coordinates are as in Figure 8 (a).

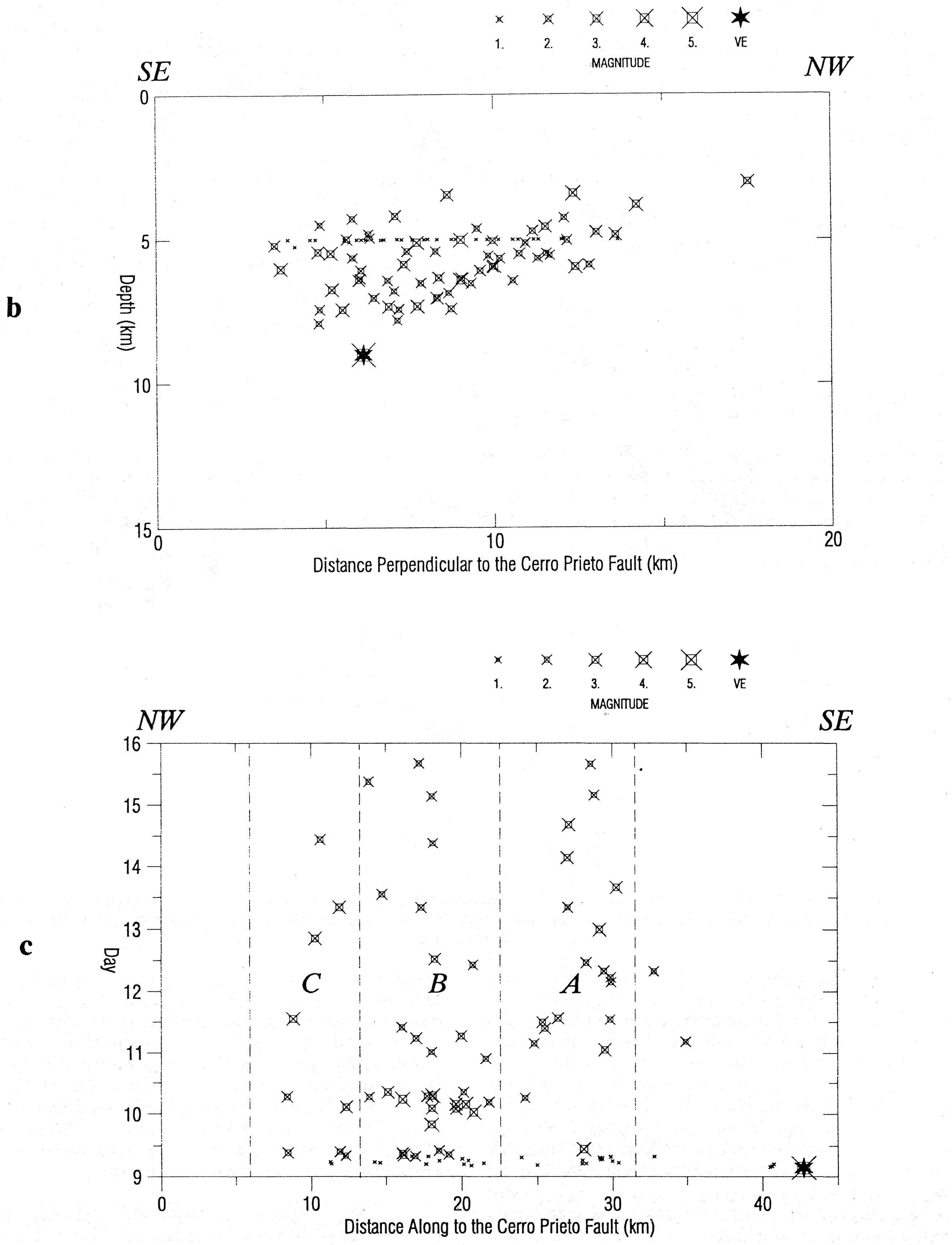
1.
2.
3.
4.
5.
VE
MAGNITUDE
SE
NW
b
Depth (km)
0
5
10
15
0
10
20
Distance Perpendicular to the Cerro Prieto Fault (km)
1.
2.
3.
4.
5.
VE
MAGNITUDE
NW
SE
c
Day
16
15
14
13
12
11
10
9
C
B
A
0
10
20
30
40
Distance Along to the Cerro Prieto Fault (km)

Fig. 8. (Cont.)

a

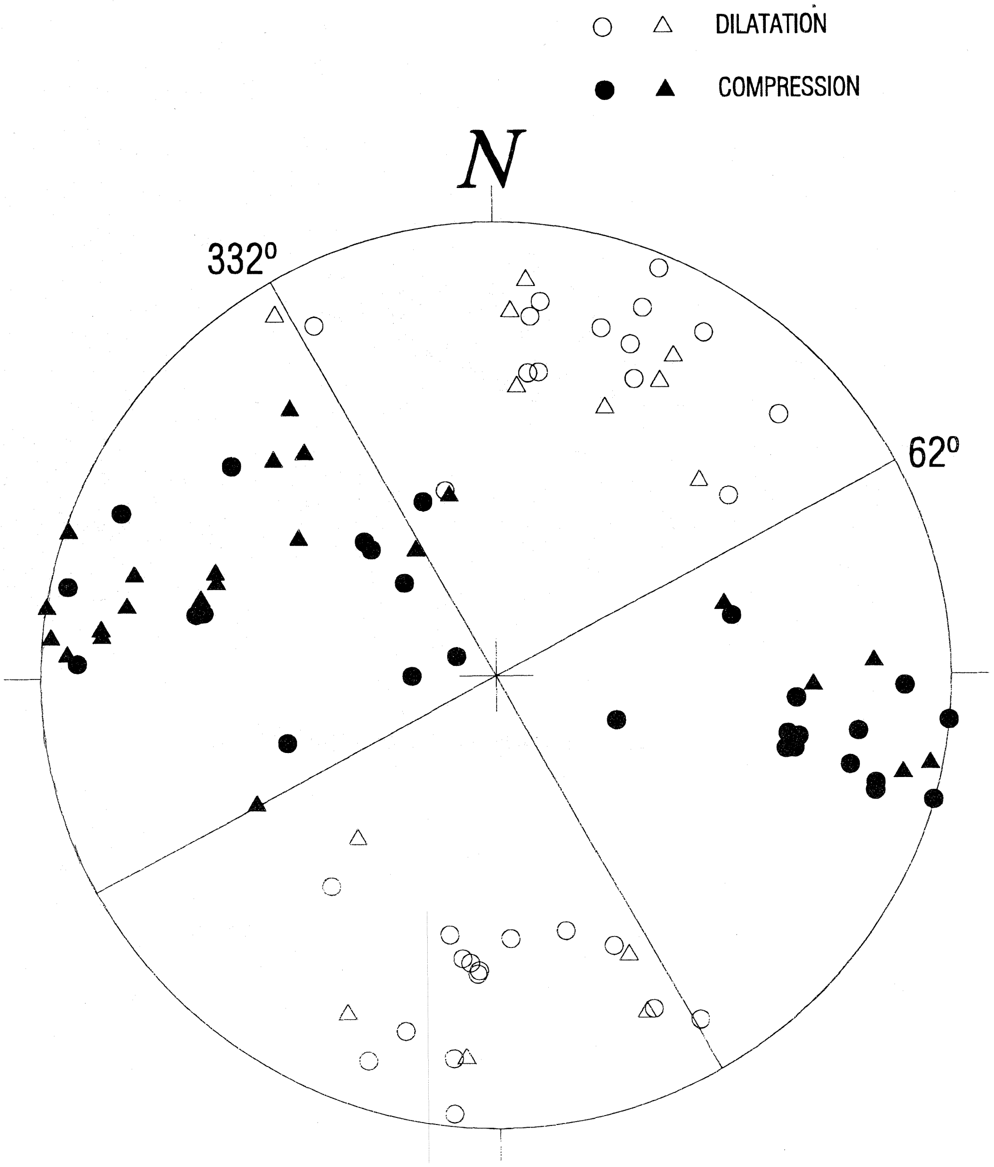

Fig. 9. Composite focal mechanisms (lower hemisphere) of aftershocks regions A (Fig. 9a) and B (Fig. 9b). Regions are as defined in Figure 4. Solid symbols, compression; open symbols; dilatations. Triangles correspond to small-amplitude of uncertain observations.

The main event triggered an aftershock sequence which clustered in time and space at the northwest end of the Cerro Prieto fault; it did not produce any significant activity after the first 24 hours in the immediate neighborhood of the main event location (less than about 10 km) or southward. We tested this conclusion by checking S-P time differences for all aftershocks recorded at local stations. As for the suggested increase of average depth of the aftershocks toward the southeast, this might be related with higher temperatures near the northwest end of the fault related to local volcanic features. A relatively high p-value for the Omori relation has been associated with higher temperatures in the aftershock source volume (Kisslinger and Jones, 1991).

The main event did not produce any clear tectonic displacement at the surface; yet accelerations measured 10 km from the fault trace (station VIC) reached 1.0 g at least six times in the upward direction and once in the downward direction within 3 seconds. The horizontal acceleration peaked at 0.85 g and exceeded 0.50 g several times within an interval of approximately 9 seconds. On the other hand, the intensity in the epicentral area was moderate (about VII), whereas the value at Mexicali was V on the modified Mercalli scale. We estimated the intensities based on oral and written reports from the epicentral area.

The focal mechanism of main shock and aftershocks near the trace of the Cerro Prieto fault can be interpreted as a right-lateral strike-slip motion, probably connected with the relative motion between the Pacific and the North America plates. The aftershocks situated at the northern end

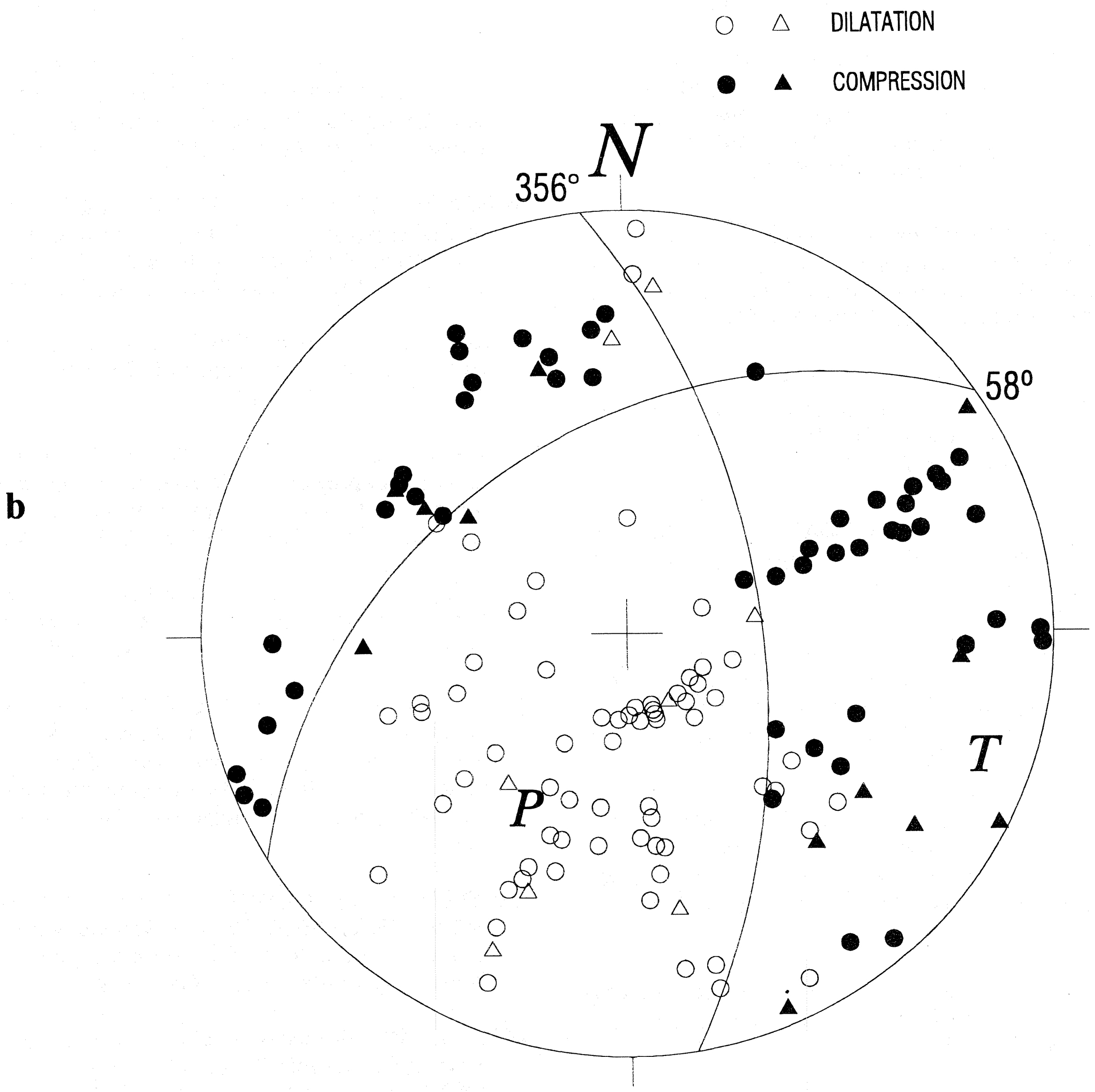

Fig. 9. (Cont.)

of the fault and those whose epicenters tend to fall toward the Imperial fault show a near-horizontal tensional axis with a NW strike, possibly related with down-thrown blocks and/or accretion of material related to local volcanic features.

ACKNOWLEDGEMENTS

Data were provided by UCSD, and CICESE. We thank M. Reichle, R. Simons, D. Chávez, J. González and A. Reyes. We appreciate the comments by R. Fernández, L. Munguía, Hubert Fabriol and the reviewers. María del Carmen and Citlali assisted with the editing. Victor Frías helped with the final editing of the figures. We used the facilities of the Computer Center at CICESE. Financial support by the Consejo Nacional de Ciencia y Tecnología de México (CONACYT) is gratefully acknowledged.

BIBLIOGRAPHY

ALBORES, A., A. REYES, J. N. BRUNE, J. GONZALEZ, L. GARCILAZO and F. SUAREZ, 1980. Seismicity studies in the region of the Cerro Prieto geothermal field. *Geothermics, 9,* 65-77.

ANDERSON, J. G., J. PRINCE, J. N. BRUNE and R. S. SIMONS, 1982. Strong Motion Accelerograms. *In:* The Mexicali Valley Earthquake of June, 1980, edited by J.G. Anderson and R.S. Simons, Newsletter of the Earthquake Engineering Research Institute, 16, 79-83.

ARCHULETA, R. J., 1982. Analysis of near-source, static, and dynamic measurements from the 1979 Imperial Valley earthquake. *Bull. Seism. Soc. Am., 72,* 1927-1956.

CHAVEZ, D., J. GONZALEZ, A. REYES, M. MEDINA, C. DUARTE, J. N. BRUNE, F. L. VERNON, R. SIMONS, L. K. HUTTON, P. T. GERMAN y C.E. JOHNSON, 1982. Main shock location and magnitude determination using combined U.S. and Mexican data. *In:* The Imperial Valley, California, Earthquake of October 15, 1979, Geol. Surv. Prof. Paper, 1254, Washington D.C., 51-54.

COBOS, J.M., 1980. Informe del levantamiento de manantiales y fracturas ocasionadas por el sismo del día 8 de junio de 1980. Technical Report, Coordinadora Ejecutiva de Cerro Prieto, Baja California, México.

DARBY, D., E. NYLAND, F. SUAREZ, D. CHAVEZ, J. GONZALEZ, 1981. Strain and displacement measurements of the June 9, 1980, Victoria, Mexico Earthquake. *Geophys. Res. Lett.*, *8*, 549-511.

ELDERS, W. A., R. W. T. MELDAR, P. T. ROBINSON and S. BIEHLER, 1972. Crustal spreading in Southern California. *Science*, *178*, 15-24.

FREZ, J., 1982. Main shock location and focal mechanism. *In:* The Mexicali Valley Earthquake of June, 1980, edited by J.G. Anderson and R.S. Simons, Newsletter of the Earthquake Engineering Research Institute, 16-3, 74-76.

FREZ, J., V. WONG and D. CHAVEZ, 1983. Interpretación de arribos secundarios en el Valle Mexicali-Imperial, Extended Abstract, Annual Meeting of the Unión Geofísica Mexicana, May 16-20, Mexico City,1555-1558.

FREZ, J. and J. GONZALEZ, 1987. Sismicidad y mecanismos focales en el Valle Mexicali-Imperial, *Geofís. Int.*, *28*, *4*, 643-691.

FREZ, J. and J. GONZALEZ, 1990. Crustal structure and seismotectonics of Northern Baja California, Chapter 15. *In:* The Gulf and Peninsular Province of the Californias, AAPG Memoir 47, edited by J.P. Dauphin and B.R.T. Simoneit, 261-283.

FUIS, S. G., W. D. MOONEY, J. H. HEALEY, G. A. McMECHAN, W. J. LUTTER, 1982. Crustal structure of the Imperial Valley region. *In:* The Imperial Valley, California, Earthquake of October 15, 1979. U.S. Geol. Surv. Prof. Paper, 1254, Washington, D.C., 25-49.

GONZALEZ, J., J. FREZ and V. WONG, 1983. Mapeo de Vp/Vs en la zona sísmica del Valle de Mexicali. *In:* Memorias VI Congreso Nacional de Ingeniería Sísmica, México, D.F., Soc. Nac. Ing. Sis., 133-149.

JOHNSON, C. E., 1979. Seismotectonics of the Imperial Valley of Southern California, Ph.D. Thesis, California Institute of Technology. Pasadena, California, 353 pp.

JOHNSON, C. E. and D. P. HILL, 1982. Seismicity of the Imperial Valley. *In:* The Imperial Valley, California, Earthquake of October 15, 1979. Geol. Surv. Prof. Paper, 1254, Washington, D.C., 15-24.

JOHNSON, C. E. and L. K. HUTTON, 1982. Aftershocks and prearthquake seismicity. *In:* The Imperial Valley, California, Earthquake of October 15, 1979, Geol. Surv. Prof. Paper, 1254, Washington, D.C., 59-76.

KISSLINGER, C. and L. JONES, 1991. Properties of aftershock sequences in Southern California. *J. Geophys. Res.*, *96*, 11947-11958.

LEE, W.H.K. and J.C. LAHR, 1975. HYPO-71 (Revised): A computer program for determining hypocenter, magnitude and first motion pattern of local earthquakes. U.S. Geol. Surv. Open-File Rep. 75-311, 114 pp.

LESAGE, P. and J. FREZ, 1990. Source parameters from body waveform data for the Victoria, Mexico, earthquake of June 9, 1980, *Geofís. Int.*, *29*, 149-169.

LISOWSKI, M. and W. H. PRESCOTT, 1982. Deformation near the epicenter of the 9 June 1980, M_L=6.2, Victoria, Mexico, Earthquake. *In:* Proceeding Fourth Simposium on Cerro Prieto Geothermal Field, Baja California, Mexico, Guadalajara, Jal., Mexico, 285-291.

LOMNITZ, C., F. MOOSER, C. ALLEN, J. N. BRUNE and W. THATCHER, 1970. Seismicity and tectonics of the Northern Gulf of California region, Mexico. Preliminary results. *Geofís. Int.*, *10*, 37-48.

MORI, J., 1991. Estimates of velocity structure and source depth using multiple P waves from aftershocks of the 1987 Elmore Ranch and Supertition Hills, California earthquakes. *Bull. Seism. Soc. Am.*, *81*, 508-523.

MUNGUIA, L. and J. N. BRUNE, 1984. Local magnitude and sediment amplification observations from earthquakes in the northern Baja California-southern California region. *Bull. Seism. Soc. Am.*, *74*, 107-119.

NAKANISHI, I. and H. KANAMORI, 1982. Effects of lateral heterogencity and source process time on the linear moment tensor inversion of long-period Rayleigh waves. *Bull. Seism. Soc. Am.*, *72*, 2063-2080.

NICHOLSON, C. and D. W. SIMPONS, 1985. Changes in Vp/Vs with depth: implications for appropiate velocity models, improved earthquake locations, and material properties of the upper crust. *Bull. Seism. Soc. Am.*, *75*, 1105-1123.

SIMONS, R. S., 1982. The strong motion record from station Victoria. *In:* The Mexicali Valley Earthquake of

June 9, 1980, edited by J.G. Anderson and R. S. Simons, Newsletter of the Earthquake Engineering Research Institute, 16-3, 83-87.

SUAREZ, F., K. E. SIEH and W. E. ELDERS, 1982. A review of geological effects and damage distribution of the June 9, 1980, Mexicali Valley earthquake. *In:* The Mexicali Valley Earthquake of June 9, 1980 edited by J.G. Anderson and R.S. Simons, Newsletter of the Earthquake Engineering Research Institute, 16-3, 99-105.

WALD, L. A., S. PERRY-HANSTON and D. D. GIVEN, 1994. The Southern California Network Bulletin: January-December 1983, Open-file Report 94-199, U. S. Geological Survey, California, U.S.A., 16 pp., and apendixes.

WEAVER, C. S. and D. P. HILL, 1978/1979. Earthquake swarms and local crustal spreading along major strike-slip faults in California. *Pageoph., 117*, 51-64.

WONG, V. and J. FREZ, 1982. Aftershock location and fault mechanisms. *In:* The Mexicali Valley Earthquake of June 9, 1980, edited by J.G. Anderson and R. S. Simons, Newsletter of the Earthquake Engineering Research Institute, 16-3, 76-79.

ZELWER, R. and R. B. GRANNELL, 1982. Correlation between precision gravity and subsidence measurements at Cerro Prieto. *In:* Proceedings of Fourth Symposium on Cerro Prieto Geothermal Field, Baja California, México, Guadalajara, Jal., Mexico, 233-241.

V. Wong, J. Frez and F. Suárez
Earth Sciences Division
CICESE,
Km. 107, Carretera Tijuana-Ensenada,
22860 Ensenada, B.C., México.